Journal of Membrane Science xxx (2011) xxx–xxx

Contents lists available at ScienceDirect

Journal of Membrane Science

journal homepage: www.elsevier.com/locate/memsci

Gas permeability reduction in PEEK film: Comparison of tetrahedral amorphous carbon and titanium nanofilm coatings

Negin Amanat[a,b,*], Alexander F. Nicoll[c], Andrew J. Ruys[c], David R. McKenzie[a], Natalie L. James[b]

[a] School of Physics, University of Sydney, NSW 2006, Australia
[b] Cochlear Ltd, 1 University Ave, Macquarie University, NSW 2109, Australia
[c] School of Aerospace, Mechanical and Mechatronic Engineering, University of Sydney, NSW 2106, Australia

ARTICLE INFO

Article history:
Received 21 February 2011
Received in revised form 9 May 2011
Accepted 9 May 2011
Available online xxx

Keywords:
PEEK
Permeability
Thin film coating

ABSTRACT

The reduction of helium gas permeability through polyetheretherketone (PEEK) microfilm (250 μm) coated with titanium (Ti) or tetrahedral amorphous carbon (ta-C) nanofilm was investigated. Two morphologies of PEEK film were used (amorphous and semi-crystalline), and four thicknesses of nanofilm were deposited (5, 20, 50, or 100 nm). Both types of nanofilm coatings reduced the overall permeability of the PEEK film, with the greatest permeability reduction of ~83% seen for the 100 nm Ti coating on semi-crystalline PEEK. Defects were identified in both types of coating; however the nature of the defects was different. The ta-C coatings exhibited a network of microcracks, while pinholes were present in the Ti coatings. The defects in both coatings were considered the dominant path for gas flow. Overall, Ti performed better than ta-C with regard to permeability reduction, and Ti also demonstrated a correlation between coating thickness and permeability reduction.

1. Introduction

The poor gas barrier properties of polymers are a limiting factor for their use in a number of applications. In the medical and electronic device industries, there has been an ongoing shift from metallic to polymer materials due to the advantages polymers offer. A key area in which polymers could have a major impact is in the protective packaging of implantable electronics. The advantages of polymers over metals include cost effectiveness, ease of fabrication (injection moldability) and design flexibility. However, for polymers to be successful in replacing metals, it is necessary to improve their barrier properties to gases and vapours [1].

In this study, thin film coatings are investigated for improving the barrier properties of polyetheretherketone (PEEK). PEEK is a thermoplastic semi-crystalline polymer used in a number of high-end applications which demand durability and robustness. Superior performance properties of PEEK include its high thermal stability (T_m = 343 °C), high mechanical strength, stiffness, fatigue and wear resistance, and excellent resistance to chemical degradation. PEEK has gained interest over the last decade for a number of implantable medical applications [2]. Its desirable properties make it a good candidate for protective encapsulation of implantable electronic components.

High gas barrier properties can be achieved by modifying the polymer surface by depositing thin film coatings such as diamond-like carbon (DLC) or metal. The metallisation of polymer membranes is common practice in the food packaging industry to keep food fresh for longer. Aluminium coatings are the most common metal coating used in the food industry [3]. The use of aluminium in medical applications has been limited as it is not considered biocompatible. Titanium is a viable alternative as it is biocompatible and already a material of choice in the dental and orthopaedic fields. Titanium thin film coatings on polymers have been investigated to improve the biocompatibility of medical polymers, such as for orthopaedic polymer implants to promote bone adhesion [4]. Metallised coatings, however, have some drawbacks depending on the application; in food packaging this can be their non-transparency. Diamond-like carbon coatings have been utilised as an alternative, for example to coat PET soft drink bottles [5]. Diamond-like carbon coatings also have applications in the biomedical field due to their biocompatibility, low friction coefficient, high wear resistance, high hardness, excellent corrosion resistance and excellent tribological properties [5,6].

Research which specifically investigates the improvement of gas barrier properties of PEEK polymer is scarce. Coating of PEEK with either DLC [6,7] or Ti [4] has been used to improve the surface properties such as biocompatibility, but the effect of the coating on gas barrier properties has not been adequately explored. Valentini et al.

* Corresponding author at: School of Physics, University of Sydney, Sydney, NSW 2006, Australia. Tel.: +61 2 9428 6213; fax: +61 2 9428 6213.
E-mail address: negin.amanat@sydney.edu.au (N. Amanat).

0376-7388/$ – see front matter © 2011 Elsevier B.V. All rights reserved.
doi:10.1016/j.memsci.2011.05.019

[7] reported gas permeation properties through amorphous hydrogenated carbon (a-C:H) coatings deposited on PEEK foils. There was an overall reduction in helium permeability; however the barrier efficiency was seen to decrease as the a-C:H film density increased; this was attributed to intrinsic stresses and the formation of a network of microcracks in the denser coatings. Hydrogenated carbon coatings, such as a-C:H, tend to be softer and more susceptible to wear than non-hydrogenated carbon coatings such as tetrahedral amorphous carbon (ta-C); this has been attributed the higher proportion of sp^3 networks in ta-C, which improve its overall hardness, wear resistance and adhesion compared to a-C:H [8]. For the application as a protective housing, where robustness is required in addition to superior barrier properties, ta-C coating may be more desirable.

The permeability of ta-C or Ti thin film coatings on PEEK has not been investigated. Development of treatments to effectively reduce the permeability of gases and water vapour through PEEK will allow its applications to be further expanded. The present study assesses and compares ta-C and Ti coatings on PEEK film and the corresponding reduction of helium permeability.

2. Methods

2.1. Materials and sample preparation

Two morphologies of untreated PEEK film (Victrex, Lacashire, UK) 250 μm thick were used as the base material in this study; amorphous (250a) and semi-crystalline (250c). The PEEK film was coated with ta-C or Ti at four different thicknesses (5, 20, 50 or 100 nm). Filtered cathodic vacuum arc (FCVA) was used as the deposition technique (Nanofilm Technologies International, Singapore). The ta-C and Ti nanofilms were produced by a FCVA system equipped with a double bend off-plane (DBOP) filter. The substrate holder was rotated during the deposition process to improve uniformity of the coating. The nanofilms were prepared using a negative substrate bias of 120 V with an arc current of 30 A for ta-C and 100 A for Ti at room temperature and a pressure of 1×10^{-5} Torr. The characteristics of all the specimens investigated in this paper are listed in Table 1.

2.2. Helium gas permeability measurements

The helium flux J (mol/m^2 s) and permeation coefficient K m^3(STP) m/m^2 Pa s) for the transport of helium through the films were determined using the experimental set up shown in Fig. 1a. A permeability chamber was custom-made to house the PEEK films (Fig. 1b), and designed to attach to the inlet port of a helium leak detector (Adixen ASM 142D). The film samples listed in Table 1 were cut into disc samples (60 mm diameter) and were secured between two O-rings; the surface area of the film samples exposed to helium was ~1134 mm^2. The film separated two compartments within the chamber; one compartment was filled with a helium–argon gas mixture (5% He and 95% Ar) under constant pressure P_{total} (400 mbar), the partial pressure of helium P_{He} was therefore 20 mbar. The other compartment was maintained under vacuum. The gas leakage rate was detected by the helium detector as a function of time, until it reached a steady state and a saturation value for the helium volumetric flow rate J' (mbar L/s) was attained. The Adixen helium leak detector is calibrated to measure helium using a 100% helium gas source. Therefore when utilising gas mixes with a lower concentration of helium, a correction factor based on the percentage content of helium must be included. In this study a 5% helium mix was used, and therefore the measured steady-state flow rate J' was multiplied by 20 to give the true helium leak rate.

To validate the permeability chamber, two tests were conducted. In the first test a steel plate (250 μm), instead of PEEK film, was used to confirm that there were no gas leaks via other pathways (e.g. the seals) other than through the film. No helium was detected when the steel plate was inserted, indicating that all helium measurements were a result of permeation through the film samples. In the second test, the helium flow rate of uncoated semi-crystalline PEEK samples of 250 μm and 500 μm thickness was measured. The measured flow rate for the 500 μm films was consistently half the flow rate of the 250 μm films, due to the linear relationship between flow rate and film thickness.

2.3. Diffusion coefficient calculations

Fick's 1st law of diffusion was used to determine the permeability coefficient of PEEK for helium:

$$J = -k\frac{\Delta P}{\Delta x} \tag{1a}$$

where J is the flux of gas through the film (mol/m^2 s), K is the permeability coefficient (m^3(STP) m/m^2 Pa s), Δx is the film thickness and ΔP is the difference in pressure of the gas across the membrane. The flux, which is the amount of helium passing through the PEEK film per unit time, can be determined from the following equation:

$$J = \frac{J'}{A \times R \times T} \tag{1b}$$

where J' is the saturated helium volumetric flow rate directly measured by the helium leak detector as volume (litres) per second measured at 1 mbar (mbar L/s). (Note: Due to the 5% helium gas mix used, the directly measured helium leak rate was multiplied by 20 to give the true J'.) A is the surface area of film the gas passes through (m^2), T is the temperature in kelvins (K), and R is the universal gas constant (83.14 L mbar/K mol). The change in pressure was approximated as P_{He} (20 mbar), since the pressure on the permeate side P_P is very small relative to that of the input pressure ($\Delta P = P_{He} - P_P \cong P_{He}$). The final units adopted for the permeability coefficient K (m^3(STP) m/m^2 Pa s) and the flux J (mol/m^2 s) are based on the recommendations given by Ehrlich [9].

2.4. Scanning electron microscopy (SEM)

After permeability measurements, the films were removed from the permeability chamber and a small disc approximately 8 mm diameter was cut from the centre of the sample. The samples were then mounted on aluminium SEM stubs using double sided conductive tape. The samples were sputter coated with platinum using a sputter coater (K550X, Quorum Emitech, UK), at 25 mA for 2 min giving a platinum coating thickness of approximately 8 nm. SEM imaging was conducted using a Zeiss Ultra plus at an accelerating voltage of 15 kV.

2.5. Nanoindentation

The hardness H and elastic modulus E of the 100 nm ta-C and Ti coatings were measured using a commercially available nanoindenter (TI 900 TriboIndenter, Hysitron Inc). Nanoindentation measurements were conducted using a Berkovich diamond indenter. A closed-loop load control function was used; indentations were performed to a peak load value of 125 μN at a loading and unloading rate of 20 μN/s, with a 2 s hold time at the peak load to account for stress relaxation. Values for H and E were calculated from the unloading curve using the Oliver and Pharr method [10]. Nine indentations were averaged per sample to obtain mean H and E values.

Please cite this article in press as: N. Amanat, et al., Gas permeability reduction in PEEK film: Comparison of tetrahedral amorphous carbon and titanium nanofilm coatings, J. Membr. Sci. (2011), doi:10.1016/j.memsci.2011.05.019

Table 1
Designation and characteristics of specimens.

Sample details	Coating thickness (nm)	Coating	Abbreviation
Amorphous PEEK control	–	–	250A
Semi-crystalline PEEK control	–	–	250C
Amorphous PEEK with 5 nm Ti	Ti	5	250A_T5
Amorphous PEEK with 20 nm Ti	Ti	20	250A_T20
Amorphous PEEK with 50 nm Ti	Ti	50	250A_T50
Amorphous PEEK with 100 nm Ti	Ti	100	250A_T100
Semi-crystalline PEEK with 5 nm Ti	Ti	5	250C_T5
Semi-crystalline PEEK with 20 nm Ti	Ti	20	250C_T20
Semi-crystalline PEEK with 50 nm Ti	Ti	50	250C_T50
Semi-crystalline PEEK with 100 nm Ti	Ti	100	250C_T100
Amorphous PEEK with 5 nm ta-C	ta-C	5	250A_C5
Amorphous PEEK with 20 nm ta-C	ta-C	20	250A_C20
Amorphous PEEK with 50 nm ta-C	ta-C	50	250A_C50
Amorphous PEEK with 100 nm ta-C	ta-C	100	250A_C100
Semi-crystalline PEEK with 5 nm ta-C	ta-C	5	250C_C5
Semi-crystalline PEEK with 20 nm ta-C	ta-C	20	250C_C20
Semi-crystalline PEEK with 50 nm ta-C	ta-C	50	250C_C50
Semi-crystalline PEEK with 100 nm ta-C	ta-C	100	250C_C100

3. Results and discussion

Fig. 2 shows the experimentally measured helium volumetric flow rate J' for each sample listed in Table 1. The results are divided into three sections for ease of interpretation: at the left are the results for the two controls (250A and 250C), in the centre the Ti coatings (for all thicknesses and both morphologies), and at the right the ta-C coatings (for all thicknesses and both morphologies). Table 2 lists the values of the helium diffusion flux (Eq. (1b)) and the calculated permeability coefficient (Eq. (1a)) for each sample.

3.1. Helium gas permeability of uncoated amorphous and semi-crystalline PEEK

The permeability of the untreated amorphous PEEK (250A) was double the semi-crystalline PEEK (250C). Semi-crystalline polymers exhibit lower permeability than their amorphous

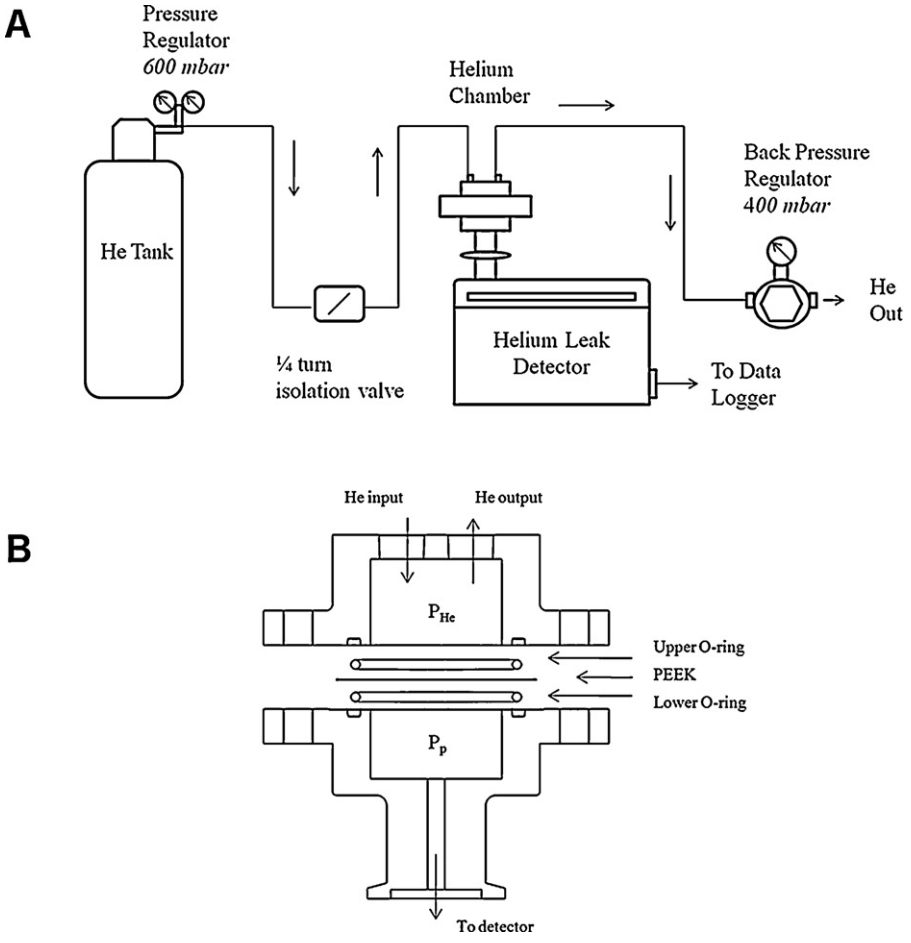

Fig. 1. (a) Schematic diagram of helium gas permeation apparatus used for helium flow rate measurements; (b) The key components of the permeability chamber. Helium that permeates through the film into the lower compartment is detected by the helium leak detector.

Please cite this article in press as: N. Amanat, et al., Gas permeability reduction in PEEK film: Comparison of tetrahedral amorphous carbon and titanium nanofilm coatings, J. Membr. Sci. (2011), doi:10.1016/j.memsci.2011.05.019

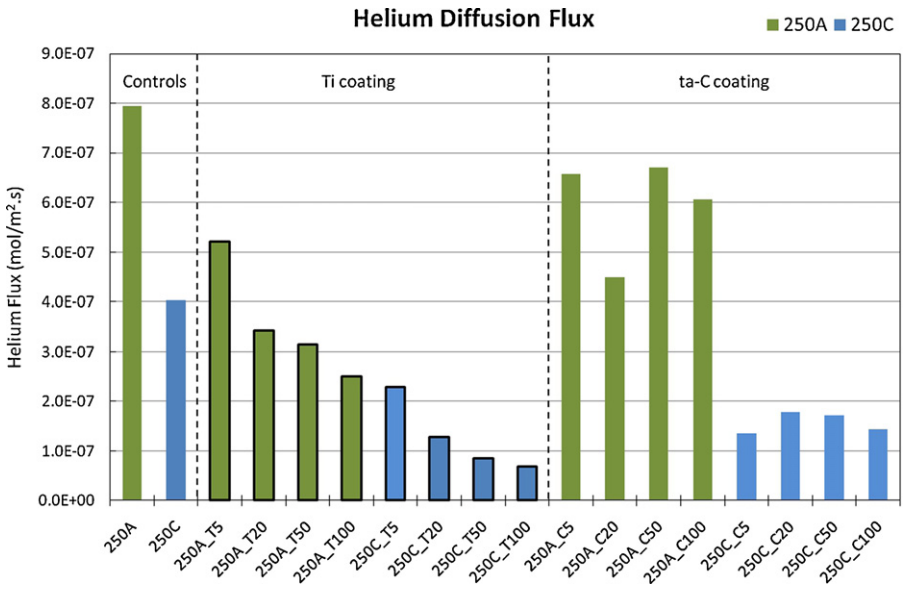

Fig. 2. Steady-state helium flux (mol/m^2 s) through the film samples listed in Table 1. Blue: 250C films; Green: 250A films. (For interpretation of the references to colour in this figure legend, the reader is referred to the web version of the article.)

counterparts. The crystalline portions of a polymer are considered essentially impermeable, however, the permeate is able to diffuse via the interconnected amorphous regions which are still present in semi-crystalline polymers, even at maximum crystallinity (which never reaches 100%).

There are three steps involved in the permeation of gases and liquids through polymeric membranes: (1) sorption onto the polymer surface, (2) diffusion through the membrane along chemical or pressure gradients, and finally (3) desorption from the polymer into the atmosphere on the other side of the membrane. Diffusion is a physical process whereby gas molecules move through the polymer via free volume movement as a result of polymer chain movement. The free volume available in polymers is affected by a number of factors, which include the density and degree of crystallinity of the polymer.

3.2. Helium gas permeability of PEEK with Ti and ta-C nanofilm coating

The results indicate that gas barrier performance was improved by coating the PEEK with either ta-C or Ti nanofilms. Ti coating proved to be the most effective, with a maximum permeability reduction of 83% for the 250C_T100. As seen in Fig. 2, both amorphous and semi-crystalline morphologies with Ti nanofilm showed reductions in permeability, and the correlation between coating thickness and permeability was inversely proportional. A regression line was fitted to the semi-crystalline and amorphous data points for Ti permeability for each coating thickness, with the best trend being a power relationship; $y = 6 \times 10^{-7}x^{-0.408}$ ($R^2 = 0.9978$) for semi-crystalline and $y = 1 \times 10^{-6}x^{-0.234}$ ($R^2 = 0.9686$) for amorphous. The ta-C coating also reduced the permeability of helium, but to a lesser extent than the Ti coatings. The greatest reduction in permeability for the ta-C coating was seen for the semi-crystalline PEEK substrates, ranging from 56% to 66% reduction. Unlike the Ti coatings, no correlation between the coating thickness and permeability was observed with the ta-C nanofilms.

Images from high resolution SEM provide insight into the surface morphology of the coatings and correlation with permeability. Fig. 3 shows a network of micro-cracks which propagate across the surface of a 100 nm ta-C coating (sample 250C_C100). Fig. 3 is representative of observations of the 50 and 100 nm ta-C coatings for both 250C and 250A. The extent of the cracking in ta-C coatings at higher magnification is shown in Fig. 3c, where the coating has catastrophically cracked down to the film-polymer interface, and the section of coating appears to be flaking off. Little to no surface cracking was observed for the thinner (5 and 20 nm) ta-C coatings at these magnifications. A study by Sheeja et al. [11] investigating the effect of film thickness on the intrinsic stress and adhesion of FCVA-deposited ta-C on silicon substrates indicated that stress within the coating increases with increasing coating thickness. This increasing level of intrinsic stress results in micro-cracking, therefore limiting the maximum thickness for ta-C coatings, and also decreases the adhesion of the coating to the substrate, leading to possible delamination. For the Ti coatings, micro-cracking was not observed (Fig. 4), however pinholes where identified as seen in Fig. 5. Pinholes in metallised coatings are the result of contamination (such as dust particles) present on the surface of the substrate during coating, these particles subsequently dislodge, leaving behind an unmetallised "shadow" [12]. Both the Ti and the ta-C coatings exhibited defects (pinholes and micro-cracking respectively) within the coating that appeared to

Table 2
Helium flux J and permeability coefficient K for helium for the film samples listed in Table 1.

Sample	J (mol/m^2 s)	K (m^3(STP) m/m^2 Pa s)
250A	7.95×10^{-7}	4.97×10^{-13}
250C	4.02×10^{-7}	2.52×10^{-13}
250A_T5	5.21×10^{-7}	3.26×10^{-13}
250A_T20	3.43×10^{-7}	2.14×10^{-13}
250A_T50	3.14×10^{-7}	1.96×10^{-13}
250A_T100	2.50×10^{-7}	1.56×10^{-13}
250C_T5	2.29×10^{-7}	1.43×10^{-13}
250C_T20	1.29×10^{-7}	8.04×10^{-14}
250C_T50	8.57×10^{-8}	5.36×10^{-14}
250C_T100	6.86×10^{-8}	4.29×10^{-14}
250A_C5	6.57×10^{-7}	4.11×10^{-13}
250A_C20	4.50×10^{-7}	2.81×10^{-13}
250A_C50	6.71×10^{-7}	4.20×10^{-13}
250A_C100	6.07×10^{-7}	3.79×10^{-13}
250C_C5	1.36×10^{-7}	8.48×10^{-14}
250C_C20	1.79×10^{-7}	1.12×10^{-13}
250C_C50	1.71×10^{-7}	1.07×10^{-13}
250C_C100	1.43×10^{-7}	8.93×10^{-14}

Please cite this article in press as: N. Amanat, et al., Gas permeability reduction in PEEK film: Comparison of tetrahedral amorphous carbon and titanium nanofilm coatings, J. Membr. Sci. (2011), doi:10.1016/j.memsci.2011.05.019

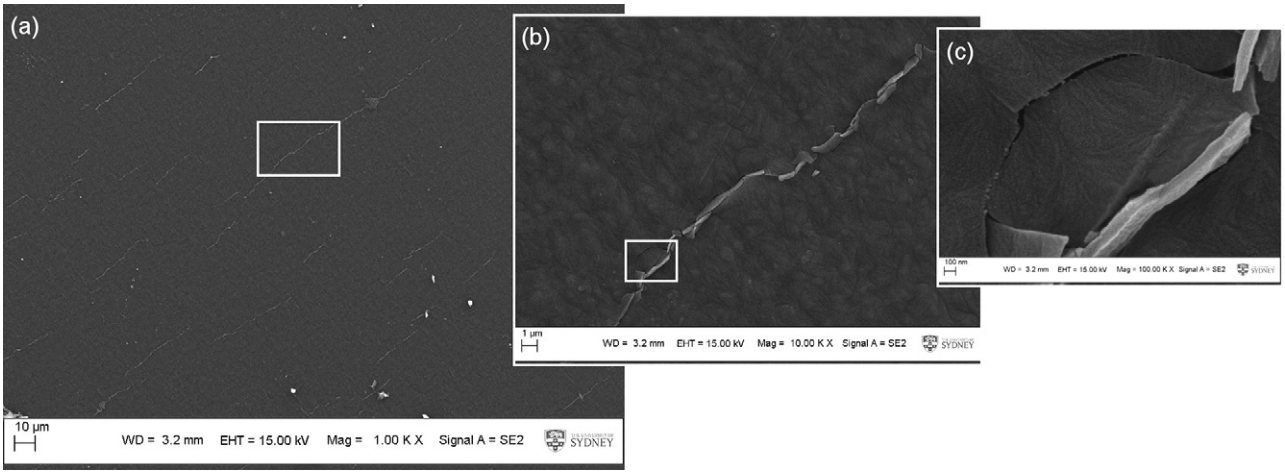

Fig. 3. SEM of 250C_C100: (a) Network of micro-cracks evident across the surface; (b) and (c) show magnified regions as indicated by the white boxes; (c) At higher magnification, brittle cracking and flaking of the coating are clearly evident.

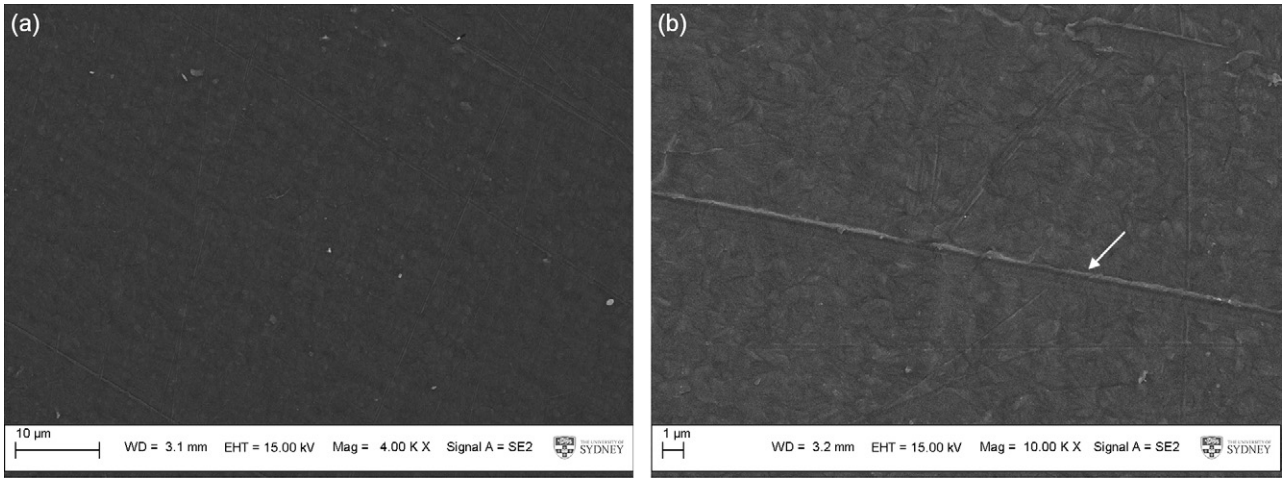

Fig. 4. SEM of 250C_T100 at two magnifications. Microcracks, as seen in the ta-C coatings, were not evident in the Ti coatings. The arrow indicates a manufacturing line in the original PEEK substrate (b) and is not a characteristic of the coating.

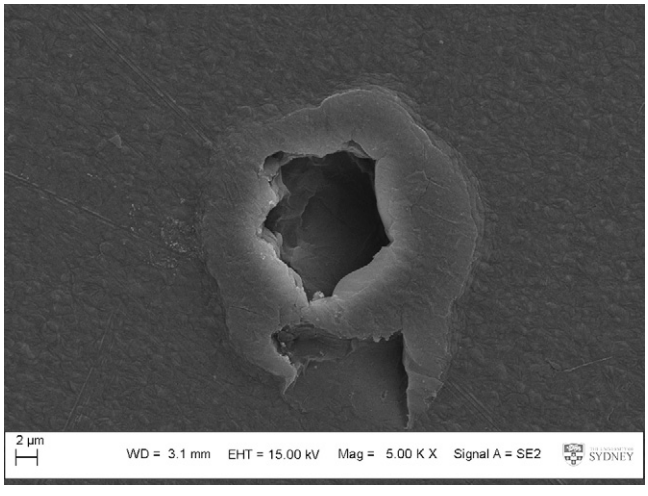

Fig. 5. SEM of sample 250C_T100 showing a pinhole in the coating.

increase in severity with coating thickness. The micro-cracking in the ta-C coatings and the pinholes in the Ti coatings provide a direct path for helium molecules to flow through to the underlying substrate.

3.3. Nano-mechanical properties of Ti and ta-C coatings

By qualitative observation, the thin film coatings appeared to have no affect on flexibility of the PEEK substrate, for all coating thicknesses. Evaluation of nanomechanical properties of thin films can be difficult due to the influence of the underlying substrate. A generally accepted method is to measure properties within an indentation depth of less than 1/10 of the film thickness in order to attain results that are substrate independent. However, for films with a thickness of 100 nm or less, accuracy within this range is difficult to achieve. We therefore measured the properties at a contact depth of 50% of the coating thickness (≈50 nm for the 100 nm coating thickness); this provided a method for comparison of mechanical properties of the film-substrate composite for the two nanofilm materials [13].

Fig. 6 shows the hardness and Young's modulus values determined for the 100 nm ta-C and Ti nanofilms. The superior gas barrier properties for the Ti coatings compared to the ta-C coatings can be explained in terms of the coating mechanical properties. The hardness of the ta-C coatings were 9-fold and 12-fold greater than the Ti coatings for the amorphous and semi-crystalline morphologies, respectively (Fig. 6). These results suggest that the ta-C films were more brittle than the Ti films, leading to the generation of micro-cracks as seen on the film surfaces in Fig. 3.

Please cite this article in press as: N. Amanat, et al., Gas permeability reduction in PEEK film: Comparison of tetrahedral amorphous carbon and titanium nanofilm coatings, J. Membr. Sci. (2011), doi:10.1016/j.memsci.2011.05.019

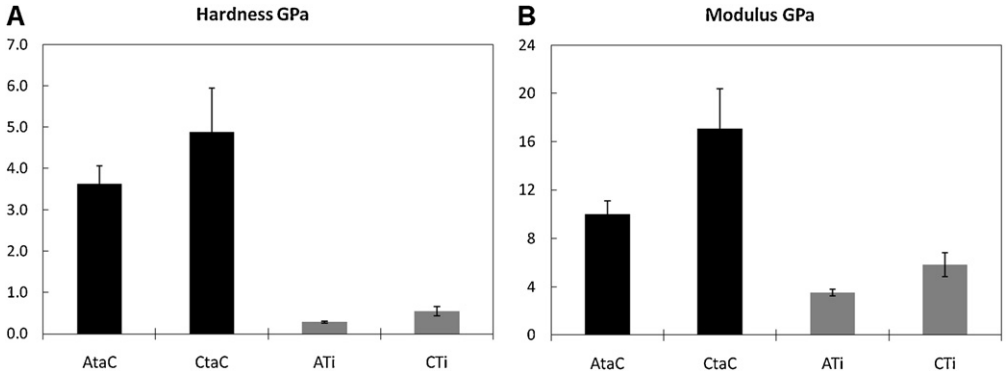

Fig. 6. Nanomechanical properties of Ti and ta-C coatings (100 nm) on amorphous and semi-crystalline PEEK substrates.

The gas barrier performance properties of carbon-based coatings with relation to nano-mechanical properties have been investigated by many researchers. A study by Abbas et al. [13] investigated reducing the high level of compressive stress in amorphous carbon coatings using silicon doping. Both ta-C and a-C:H coatings were investigated on polyethylene terepthalate (PET) and polycarbonate (PC) substrates. Silicon doping was shown to significantly improve the gas barrier properties of both coating types due to an improvement in surface morphology as a result of stress relaxation in the coating. Both ta-C and a-C:H coatings were covered by a network of microcracks; these microcracks disappeared when doped with silicon. A similar approach could be adopted to reduce the intrinsic stresses of carbon coatings on PEEK substrates.

3.4. Diffusion mechanisms through nanofilm coatings – dependence on substrate morphology and coating thickness

A clear disparity in gas permeability was observed between the amorphous and semi-crystalline morphologies of PEEK substrates which had the same nanofilm coating and thickness. Furthermore, the effect of coating thickness on permeation for the ta-C and Ti coatings was completely different, with Ti showing a clear relationship, while ta-C appeared to have no relationship.

In order to interpret the results, the mechanisms of gas transport through materials require discussion. Two different mechanisms of gas transport through materials can occur: (1) bulk diffusive flow often referred to as the solubility-diffusion mechanism (as discussed in Section 3.1), and (2) flow through defects in the material (which include pinholes and microcracks). The latter mechanism can significantly alter results, such that the flow through defects in a coating may be many times greater than flow via diffusion, potentially making diffusive flow negligible; the permeability reduction of a polymer is thus solely dependent on the frequency and size of defects in the coating. Moreover, the permeation flow rate for the solubility-diffusion mechanism is inversely proportional to the coating thickness, whereas the flow through defects is independent of thickness [14,15]. In the present study, it is therefore likely that helium flow via the defect path was the dominant mechanism for ta-C coatings due to lack of an effect of coating thickness. For the Ti coatings, the inverse correlation with thickness suggests that elongation of pinhole paths, thus increasing tortuosity, may have been a more prominent factor.

A review conducted by Chatham [12] assessed the results of studies investigating oxygen permeation through various metal-coated polymer systems as a function of coating thickness. The review showed that oxygen permeability decreased with increasing coating thickness, until reaching a minimum value (P_M) for coating thicknesses above a critical thickness (Λ_c). Chatham postulated that barrier effectiveness of a coating was determined solely by gas transport through defects in a metallised coating, and that the observed initial decrease in permeability (before reaching P_M) was due to the requirement for a finite coating thickness to achieve complete coverage of the polymer surface. It should be noted that gas diffusion is also dependent on the gas molecule shape and size, and permeability is dependent on the gas diffusion and gas solubility, hence different permeabilities are expected for different gases. The studies investigated by Chatham assessed oxygen permeability, and the permeabilities for oxygen and helium would not be the same, due to differences in solubility and diffusivity. However, the results of the present study reflect the trends seen in Chatham's findings; permeation through the barrier coating appeared to be dominated by flow through defects in the coating. It is of interest to note that the Ti coating followed an inverse trend with coating thickness in our study, and according to the fitted trend line discussed in Section 3.2 would reach a minimum at a critical thickness. However, as the coating thickness increased, the channels created by the pinholes effectively lengthen, therefore it is more likely that the decrease in permeability is due to increased tortuosity of the channels with thickness [16] rather than increased coverage of the coating.

It should also be noted that delamination between the coating and substrate can occur. Delamination may arise due to differences between the thermal expansion coefficients of the polymer substrate and the coating material. These interfacial gaps could reduce the barrier performance of a film, particularly if they are connected to cracks and/or pinholes.

The formation of pinholes in films deposited by physical vapour techniques such as cathodic vacuum arc deposition poses a significant challenge. A defect-free surface would greatly enhance the barrier performance of the films. One technique that may produce a pinhole free surface is atomic layer deposition (ALD) [17]. Recent advances in ALD have shown that enhanced barrier properties can be achieved for water vapour and oxygen gas transmission using 25 nm thick aluminium oxide coatings on a polyethylene napthalate [18]. Hirvikorpi et al. [19], however, demonstrated that the barrier improvement with ALD is substrate dependent, and that thicker coatings on rough substrate surfaces can lead to cracking. Further work is required to assess the suitability of the ALD technique on PEEK substrate.

4. Conclusions

We investigated the gas permeability of PEEK film coated with ta-C and Ti nanofilms to determine the level of permeability reduction that could be achieved. The following conclusions were made from the study:

Please cite this article in press as: N. Amanat, et al., Gas permeability reduction in PEEK film: Comparison of tetrahedral amorphous carbon and titanium nanofilm coatings, J. Membr. Sci. (2011), doi:10.1016/j.memsci.2011.05.019

- Ti or ta-C coatings applied to PEEK reduced the permeability to helium; the maximum reduction in permeability of 83% was achieved with a 100 nm Ti coating on semi-crystalline PEEK.
- Ti coating had superior barrier properties compared to ta-C.
- The defects in the coating layer were a governing factor for the overall gas barrier performance of PEEK film coated with either ta-C or Ti. The defects provided a direct path to the underlying substrate, therefore making the resultant gas permeability also dependent on substrate properties.
- Helium gas flow through ta-C was independent of coating thickness. This was attributed to the network of micro-cracks which propagated through to the underlying substrate.
- There was an inverse trend for permeability and coating thickness for the Ti coatings; this is attributed to the increased tortuosity of the pinhole channels as the coating thickness increased.

Improving the barrier properties of PEEK will expand its potential as a protective encapsulant for implantable electronic components. This study shows that coating of PEEK with a nanofilm barrier can reduce permeability by up to ~83%. Titanium coating was identified as the superior coating, compared with ta-C, but further work is required to minimise pinhole formation to decrease permeability further.

Acknowledgements

This study was supported by an Australian Research Council (ARC) Linkage Grant (LP0776313). Scanning electron microscopy was conducted at the Australian Centre for Microscopy & Microanalysis (ACMM), University of Sydney. The authors would like to thank Dr. Shi Xu of Nanofilm Technologies for generously providing the coated samples of PEEK.

References

[1] N. Amanat, N.L. James, D.R. McKenzie, Medical Engineering & Physics 32 (2010) 690–699.
[2] N. Sereno, European Medical Device Technology 1 (3) (2010).
[3] M. Ozdemir, C.U. Yurteri, H. Sadikoglu, Critical Reviews in Food Science and Nutrition 39 (5) (1999) 457–477.
[4] C.M. Han, E.J. Lee, H.E. Kim, Y.H. Koh, K.N. Kim, Y. Ha, S.U. Kuh, Biomaterials 31 (13) (2010) 3465–3470.
[5] A. Shirakura, M. Nakaya, Y. Koga, H. Kodama, T. Hasebe, T. Suzuki, Thin Solid Films 494 (1–2) (2006) 84–91.
[6] H.Y. Wang, M. Xu, W. Zhang, D.T.K. Kwok, J.A. Jiang, Z.W. Wu, P.K. Chu, Biomaterials 31 (32) (2010) 8181–8187.
[7] L. Valentini, M.C. Bellachioma, L. Lozzi, S. Santucci, J.M. Kenny, Journal of Vacuum Science & Technology A – Vacuum Surfaces and Films 20 (5) (2002) 1647–1652.
[8] P. Lemoine, J.P. Quinn, P. Maguire, J.A. McLaughlin, Wear 257 (5–6) (2004) 509–522.
[9] C.D. Ehrlich, Journal of Vacuum Science & Technology A – Vacuum Surfaces and Films 4 (5) (1986) 2384–2385.
[10] W.C. Oliver, G.M. Pharr, Journal of Materials Research 7 (6) (1992) 1564–1583.
[11] D. Sheeja, B.K. Tay, K.W. Leong, C.H. Lee, Diamond and Related Materials 11 (9) (2002) 1643–1647.
[12] H. Chatham, Surface & Coatings Technology 78 (1–3) (1996) 1–9.
[13] G.A. Abbas, S.S. Roy, P. Papakonstantinou, J.A. McLaughlin, Carbon 43 (2) (2005) 303–309.
[14] E.H.H. Jamieson, A.H. Windle, Journal of Materials Science 18 (1) (1983) 64–80.
[15] W. Prins, J.J. Hermans, Journal of Physical Chemistry 63 (5) (1959) 716–722.
[16] P. Mercea, L. Muresan, V. Mecea, D. Silipas, I. Ursu, Journal of Membrane Science 35 (3) (1988) 291–300.
[17] T. Suntola, Thin Solid Films 216 (1) (1992) 84–89.
[18] M.D. Groner, S.M. George, R.S. McLean, P.F. Carcia, Applied Physics Letters 88 (5) (2006).
[19] T. Hirvikorpi, M. Vaha-Nissi, T. Mustonen, E. Iiskola, M. Karppinen, Thin Solid Films 518 (10) (2010) 2654–2658.

Please cite this article in press as: N. Amanat, et al., Gas permeability reduction in PEEK film: Comparison of tetrahedral amorphous carbon and titanium nanofilm coatings, J. Membr. Sci. (2011), doi:10.1016/j.memsci.2011.05.019